AD _____

Award Number: W81XWH-11-1-0341

TITLE: Non-thermal high-intensity focused ultrasound for breast cancer therapy

PRINCIPAL INVESTIGATOR: Chang Ming (Charlie) Ma, Ph.D.

CONTRACTING ORGANIZATION:

          Fox Chase Cancer Center
          Philadelphia, PA 19111

REPORT DATE: July 2012

TYPE OF REPORT: Annual

PREPARED FOR: U.S. Army Medical Research and Materiel Command
          Fort Detrick, Maryland 21702-5012

DISTRIBUTION STATEMENT:
          Approved for public release; distribution unlimited

REPORT DOCUMENTATION PAGE			*Form Approved* *OMB No. 0704-0188*

Public reporting burden for this collection of information is estimated to average 1 hour per response, including the time for reviewing instructions, searching existing data sources, gathering and maintaining the data needed, and completing and reviewing this collection of information. Send comments regarding this burden estimate or any other aspect of this collection of information, including suggestions for reducing this burden to Department of Defense, Washington Headquarters Services, Directorate for Information Operations and Reports (0704-0188), 1215 Jefferson Davis Highway, Suite 1204, Arlington, VA 22202-4302. Respondents should be aware that notwithstanding any other provision of law, no person shall be subject to any penalty for failing to

1. REPORT DATE *(DD-MM-YYYY)* 01-07-2012	2. REPORT TYPE Annual	3 DATES COVERED *(From - To)* 1 Jul 2011 - 30 Jun 2012	
4. TITLE AND SUBTITLE Non-thermal high-intensity focused ultrasound for breast cancer therapy		**5a. CONTRACT NUMBER**	
		5b. GRANT NUMBER W81XWH-11-1-0341	
		5c. PROGRAM ELEMENT NUMBER	
6. AUTHOR(S) Chang Ming (Charlie) Ma, Ph.D.		**5d. PROJECT NUMBER**	
		5e. TASK NUMBER	
		5f. WORK UNIT NUMBER	
7. PERFORMING ORGANIZATION NAME(S) AND ADDRESS(ES) Fox Chase Cancer Center Philadelphia, Pennsylvania 19111		**8. PERFORMING ORGANIZATION REPORT**	
9. SPONSORING / MONITORING AGENCY NAME(S) AND ADDRESS(ES) U.S. Army Medical Research and Materiel Command Fort Detrick, Maryland 21702-5012		**10. SPONSOR/MONITOR'S ACRONYM(S)**	
		11. SPONSOR/MONITOR'S REPORT NUMBER(S)	

12. DISTRIBUTION / AVAILABILITY STATEMENT
Approved for public release; distribution unlimited

13. SUPPLEMENTARY NOTES

14. ABSTRACT

Several in vitro studies have demonstrated the non-thermal (< 42 ºC) cell killing effect of HIFU, which resembles high linear energy transfer (LET) radiation cell damage that is not affected by the local biochemical environment and shows less radiation resistance. However, there have been no in vivo animal studies performed on non-thermal HIFU to demonstrate its therapeutic potential. This project aims to demonstrate the therapeutic potential of non-thermal HIFU in vivo using an animal model by comparing it with well established treatment modalities such as radiation therapy. This project has two aims: (1) to determine if non-thermal HIFU can cause significant tumor growth delays in vivo as compared to radiation therapy using an animal breast cancer model, and (2) to determine potential normal tissue toxicities, if any, associated with non-thermal HIFU treatment for breast cancer. Extensive phantom studies have been completed to determine suitable ultrasound parameters for the in vivo animal experiments. However, the tasks planned for the animal studies were not completed due to the delayed approval of the animal protocol. A no-cost extension has been approved to complete the remaining tasks by the end of June 2013.

15. SUBJECT TERMS

HIFU, MR guidance, non-thermal effect, breast cancer

16. SECURITY CLASSIFICATION OF:			17. LIMITATION OF ABSTRACT	18. NUMBER OF PAGES	19a. NAME OF RESPONSIBLE PERSON USAMRMC
a. REPORT U	**b. ABSTRACT** U	**c. THIS PAGE** U	UU	17	**19b. TELEPHONE NUMBER**

Table of Contents

INTRODUCTION: Over the past decades there were encouraging findings from in vitro studies on the non-thermal (< 42 ºC) cell killing effect of HIFU, which resembles high linear energy transfer (LET) radiation cell damage that is not affected by the local biochemical environment and shows less radiation resistance [1-5]. However, there have been no in vivo animal studies performed on non-thermal HIFU to demonstrate its therapeutic potential. This was due to the lack of accurate HIFU treatment systems for small animal models. Advanced imaging systems will be required to determine the gross tumor volume, to plan the HIFU treatment, to monitor the treatment process, and to assess the treatment outcome in order to maximize the therapeutic effect of non-thermal HIFU on tumor cells and to minimize unnecessary damage to normal tissues. The purpose of this project is to demonstrate the therapeutic potential of non-thermal HIFU in vivo using an animal model by comparing it with well established treatment modalities such as radiation therapy.

BODY: This project has two aims: (1) to determine if non-thermal HIFU can cause significant tumor growth delays in vivo as compared to radiation therapy using an animal breast cancer model, and (2) to determine potential normal tissue toxicities, if any, associated with non-thermal HIFU treatment for breast cancer. We have defined 3 tasks for this project: (1) Determine MRI and HIFU parameters for MRgFUS treatment of breast cancer under non-thermal conditions, (2) Perform MRgFUS and radiation treatments of breast cancer using a mouse model, and (3) Analyze experimental results to establish whether non-thermal HIFU provides sufficient tumor growth inhibition compared with radiation.

To perform non-thermal HIFU treatments of breast cancer in vivo, a commercial HIFU system (InSightec ExAblate 2000) with a 1.5T MR scanner has been used to provide real-time, MR image-guided non-thermal HIFU treatment on a mouse model with solitary breast tumors. MR guided HIFU allows for selection of the optimal ultrasound beam path prior to each sonication and localization of the ultrasound focal zone with sub-millimeter accuracy. The tissue temperature can be monitored by MR thermometry during each sonication to ensure non-thermal HIFU treatment. Based on Task (1) a series of pilot experiments has been successfully carried out on both an acoustic phantom and mice implanted with human breast cancer cells (MCF-7) to determine HIFU parameters including the ultrasound frequency, acoustic power, acoustic energy, and pulse width under the MR guidance. Figure 1 shows combinations of acoustic power and ultrasound duration that resulted in safe temperature elevation in the acoustic phantom. These results have been used to guide the selection of ultrasound parameters for the in vivo experiments in Task (2) and in other experiments using the same HIFU system. Some results of this study have been published in a paper of Chen et al (2012) (see Appendices).

A study was also successfully carried out to quantify the delineation accuracy using the 1.5 T MR imaging system by comparison with the contours drawn using a 7 T Bruker MR system (see Figure 2). The results clearly demonstrated that the clinical 1.5 T MR system is sufficient for our study while commonly used caliper measurements with simple calculation methods were less accurate for measuring internal organs and structures (see Figure 3). Caliper measurements have been used successfully for superficial tumors. Adequate ultrasound parameters have been determined based on the above results to ensure the generation of intense cavitation and other non-thermal effects at normal body temperatures (< 42 ºC).
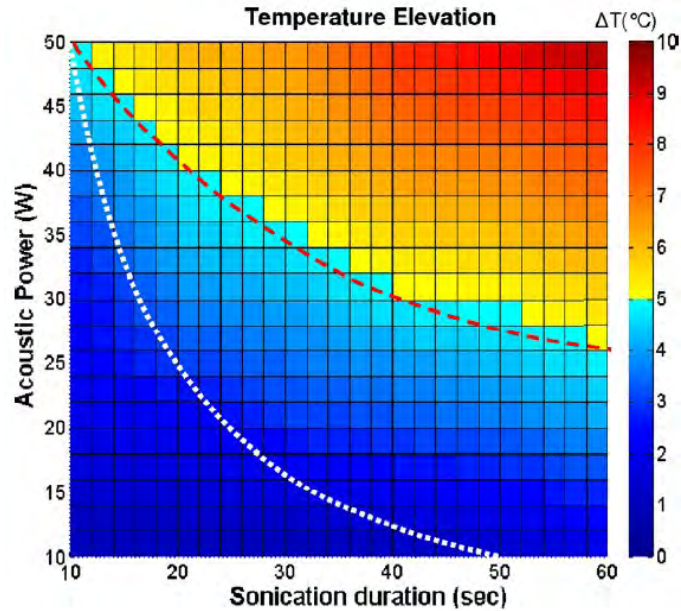
Figure 1 pFUS-induced temperature elevation using different acoustic powers and sonication durations based on the tissue phantom measurement (acoustic frequency: 1 MHz; duty cycle: 10%; pulse rate: 1 Hz). The red dashed line indicates a 5 °C temperature elevation, which will increase the body temperature to 42 °C, assuming a normal body temperature of 37 °C. The white dotted line indicates the same acoustic energy delivered using different acoustic power and the temperature elevation changes.
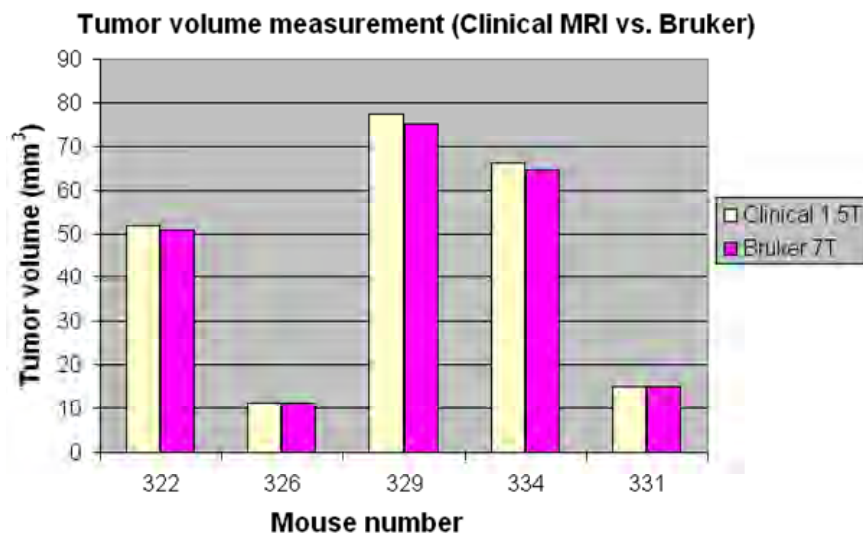
➢

Figure 2 The delineation accuracy using the 1.5 T MR imaging system by comparison with the contours drawn using a 7 T Bruker MR system for prostate tumors. The average volume difference was $1.5 \pm 0.6\%$ between the 7 T Bruker system and the 1.5 T clinical MR system.

Following these pilot studies, in vivo experiments were performed to determine the therapeutic

effect of HIFU by comparing it with radiation treatments using the same animal model as designed in Task (2). However, due to the delayed approval of our animal protocol by IACUC and ACURO we only had less than 6 months to perform our designed animal experiments. Therefore, we could not complete our Task (2) for all of the animals. We have applied for a no-cost extension for another 12 months, which was approved by the DOD with the new performance period: 1 July 2011 - 31 July 2013 (30 June 2013).
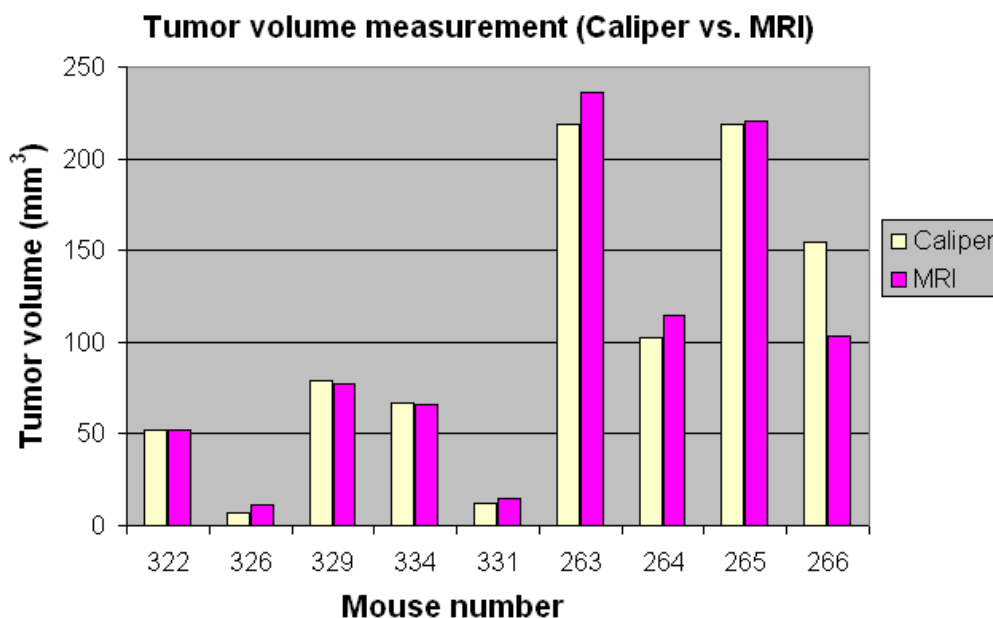

Tumor volume measurement (Caliper vs. MRI)

Figure 3 The tumor volumes measured using a caliper and a 7 T Bruker MR system. The average volume difference was $14.2 \pm 6.1\%$ between the two techniques for prostate tumors.

Although we only had limited time to perform the animal studies, we still managed to test all of the steps of our experimental procedure to ensure that the project will be completed successfully with the no-cost extension that was planned in our original Task (2) and Task (3). The following descriptions are based on the limited animal studies carried out during the first year (note that we stopped the experiment once our animal protocol expired). First, we have tested successfully our animal model. The tumor cells (0.5 ml, 1×10^7) of MCF-7 line were inoculated into the subcutaneous tissue of female BALB/c nude mice (34 tumors total) to mimic breast tumors as observed clinically. Tumor-bearing mice (2 only) were then treated using MR-guided HIFU with predetermined treatment parameters once a week for a total of 2 weeks to quantify the therapeutic effect, and to derive the biologically equivalent dose for pulsed HIFU using tumor growth delay as an end point (Figures 4 and 5). The tumor volume was measured weekly on the 1.5 T MR scanner since it provides adequate delineation accuracy. Animals were monitored and euthanized 4 weeks after the treatment. Due to the expiration of our animal protocol, we did not perform the radiation treatment yet.

Histopathological analyses were performed to evaluate normal and tumor cell damage. A study on skin damage due to non-thermal was also started (but not finished, Figure 6) and the
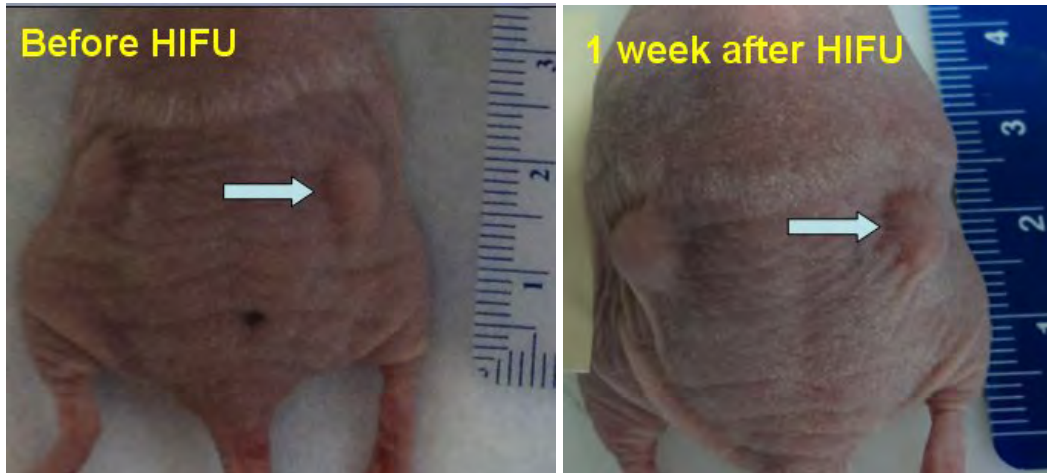
Figure 4 Photos of breast tumors treated with non-thermal HIFU with previously determined ultrasound parameters.
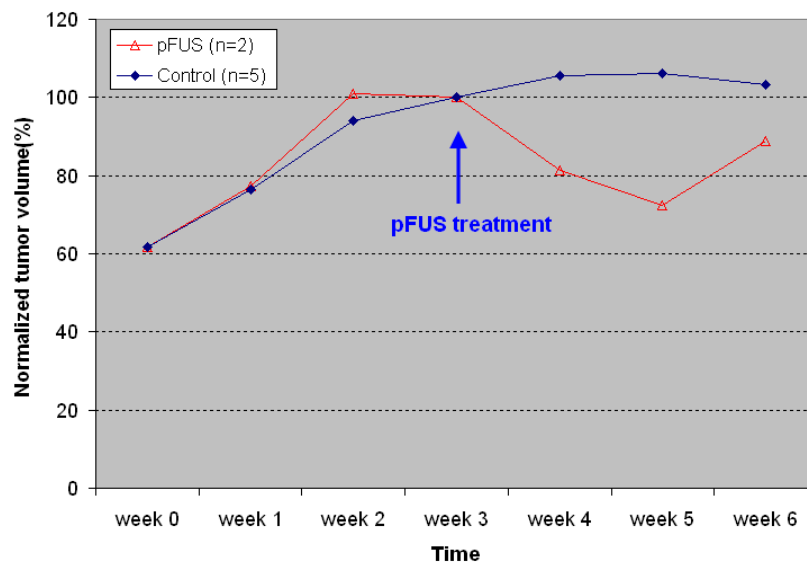

Figure 5 Comparison of tumor volumes treated with non-thermal HIFU with previously determined ultrasound parameters with the control tumors.

preliminary results showed that the skin response to HIFU exposures was temporary and reversible.

KEY RESEARCH ACCOMPLISHMENTS:

- Established an effective animal model to study non-thermal HIFU treatment of breast cancer
- Determined suitable ultrasound parameters for non-thermal HIFU treatments using in vivo animal models
- Demonstrated the measurement accuracy for tumor growth delay studies
- Tested the experimental procedures for the in vivo study

- Tested the imaging/histo-pathological methods to study the mechanisms of the non-thermal HIFU effect and its associated toxicities.
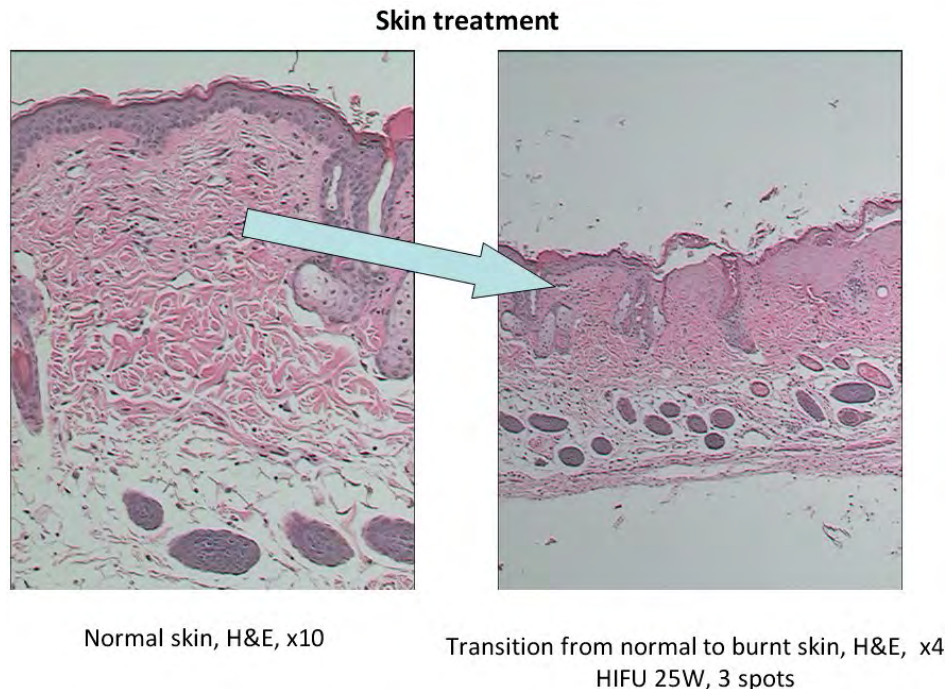
Skin treatment

Normal skin, H&E, x10

Transition from normal to burnt skin, H&E, x4
HIFU 25W, 3 spots

Figure 6 Histology study to show skin reaction to high-intensity HIFU treatment.

REPORTABLE OUTCOMES: Provide a list of reportable outcomes that have resulted from this research to include:

- 1 paper published, 1 abstract accepted for oral presentation at the national conference.
- Established an animal model for breast cancer for non-thermal HIFU study.

CONCLUSION: Although our project was delayed due to the animal protocol approval, we have completed our Task (1) to determine suitable ultrasound parameters for the non-thermal HIFU treatment of superficial breast tumors and the techniques to evaluate the tumor volume accurately for the tumor growth delay study. We have partially completed Tasks (2) and (3) and the preliminary data have demonstrated the non-thermal effect of HIFU that are likely to be used for cancer therapy. We have applied a no-cost extension for 12 months to complete the rest of the animal study in order to provide useful results with statistical significance to demonstrate the necessity for further feasibility studies and/or preclinical animal studies to determine optimal HIFU treatment parameters for human treatments and to quantify normal tissue toxicities associated with non-thermal HIFU treatments.

REFERENCES:

1. Kennedy J E, Ter Haar G R, Cranston D, High intensity focused ultrasound: surgery of the future? The British journal of radiology 2003; 76:590-9.

2. Miller D L, Tho mas R M, Buschbo m R L, Comet assay reveals D NA strand breaks induced by ultrasonic cavitation in vitro, Ultrasound in medicine & biology 1995; 21: 841-8.

3. Dalecki D, Mechanical bioeffects of ultrasound, Annu Rev Biomed Eng. 2004; 6: 229-48.

4. Feril L B, Kondo T, Cui Z-G, Tabuchi Y, Zha o Q-L; Ando H, Misaki T, Yoshika wa H, Umemura S, Apoptosis induced by the sonom echanical effects of lo w intensity pulsed ultrasound in a human leukemia cell line, Cancer letters 2005; 221: 145-52.

5. Jernberg A, Ultrasound, ions and combined modalities for increased local tumor cell death in radiation therapy, Ph.D. Thesis, Karolinska Institute, Stockholm, Sweden, 2007.

APPENDICES:

1. C-M Ma, D Cvetkovic, XM Chen, R Gupta and L Chen, Non-Therm al Effect of Pulsed High-Intensity Focused Ultrasound – an in Vivo Study, FUSF 2012 annual m eeting, Washington DC (accepted as oral presentation)

2. Xiaoming Chen, D Cvetkovic, C -M Ma an d L Chen, Quantitativ e study of focused ultrasound enhanced doxorubicin delivery to pros tate tumor in vivo with MRI guidance, Medical Physics, Vol. 39, No. 5, 2780-86, May 2012

Non-Thermal Effect of Pulsed High-Intensity Focused Ultrasound – an in Vivo Study
C-M Ma, D Cvetkovic, XM Chen, R Gupta and L Chen

Introduction: Extensive studies have been carried out on MR guided focused ultrasound (MRgFUS) for ablative therapy and drug enhancement for gene th erapy and chemotherapy by many investigators and in our institution. In this work we have conducted in vivo anim al experiments to explore the feasibility of pulse d high-intensity focused ultrasound (pHIFU) for non-thermal cancer therapy.

Methods: Phantom studies were first carried out to obtain suitable US param eters for non-thermal (below 42° C) s onications using an InSightec ExAblate 2000 system with a 1.5T GE MR scanner. Different com binations of acous tic powers and duty cycles were in vestigated, keeping the tem perature below 42° C as m easured by real-tim e MR thermom etry. Nude m ice with implanted (LNCaP) prostate and (MCF-7) breast cancers were treated with pHIFU (1 MHz; 5 & 25 W acoustic power, 0.1 & 0.5 duty cycle; 60 sec duration). Th e animals were allowed to survive for 4 weeks af ter the treatment. The tumor growth was m onitored on a 7T MR scanner and compared with the control group.

Results and Discussion: Significant tumor growth delay was observed in the m ice treated with pHIFU. The m ean tumor volume for the pHIFU treated mice was 30% and 65% sm aller than that of the control m ice for 5 W /0.5 duty cycl e and 25 W/0.1 duty cycle treatm ent settings, respectively. Histology analyses perform ed at different time points afte r the pHIFU sonication indicated non-ablative cell damage together with apoptotic/mitotic cell deaths.

Conclusion: These in vivo experim ents demonstrated that non-thermal pHIFU has a great potential for cancer therapy. Further experim ents are needed to derive optim al ultrasound parameters and fractionation schemes to m aximize the therapeu tic effect and to investigate normal tissue toxicities.

Quantitative study of focused ultrasound enhanced doxorubicin delivery to prostate tumor *in vivo* with MRI guidance

Xiaoming Chen, Dusica Cvetkovic, C.-M. Ma, and Lili Chen[a)]
Department of Radiation Oncology, Fox Chase Cancer Center, Philadelphia, Pennsylvania 19111

Purpose: The purpose of this study was to investigate the potential of MR-guided pulsed focused ultrasound (pFUS) for the enhancement of drug uptake in prostate tumors *in vivo* using doxorubicin (Dox).

Methods: An antitumor drug Dox, an orthotopic animal prostate tumor model using human prostate cancer, LNCaP cell line, and a clinical FUS treatment system (InSightec ExAblate 2000) with a 1.5T GE MR scanner were used in this study. First, experiments on a tissue mimic phantom to determine the optimal acoustic power and exposure durations with a 10% duty cycle and a 1 Hz pulse rate were performed. The temperature variation was monitored using real-time MR thermometry. Second, tumor-bearing animals were treated with pFUS. There were three groups ($n = 8$/group): group 1 received pFUS + Dox (10 mg/kg i.v. injection immediately after pFUS exposure), group 2 received Dox only (10 mg/kg i.v. injection), and group 3 was a control. Animals were euthanized 2 h after the pFUS treatment. The Dox concentration in the treated tumors was measured by quantifying fluorescent tracers using a fluorometer. Third, the histological changes of tumors with and without pFUS treatments were evaluated. Finally, experiments were performed to study the spatial drug distribution in tumors after the pFUS treatment, in which two animals received pFUS + Dox, two animals received Dox only, and one animal was used as control. Two hours following the treatment, animals were euthanized and processed. The Dox distribution was determined using a fluorescence microscope.

Results: Parametric measurements using a tissue phantom showed that the temperature increased with an increasing acoustic power (from 10 to 50 W) or sonication duration (from 10 to 60 s) with a given acoustic frequency of 1 MHz, duty cycle 10%, and pulse rate 1 Hz. A set of ultrasound parameters was identified with which the temperature elevation was less than 5 °C, which was used for nonthermal pFUS sonication. Increased Dox concentration (14.9 ± 2.5 μg/g) was measured in the pFUS-treated group compared to the Dox-only group (9.5 ± 1.6 μg/g), indicating an approximate 60% increase with $p = 0.05$. The results were consistent with the increased spatial drug distributions by fluorescence imaging. Histological analysis showed increased extravasation in pFUS-treated prostate tumors suggesting increased drug delivery with pFUS.

Conclusions: The results showed that pFUS-enhanced drug uptake in prostate tumors was significant. This increased uptake may be due to increased extravasation by pFUS. Optimal pFUS parameters may exist to maximize the drug uptake, and this study using Dox demonstrated a quantitative method for such systematic parametric studies. In addition, this study may provide useful data for the potential application of pFUS-mediated Dox delivery for prostate tumor therapy. © *2012 American Association of Physicists in Medicine*. [http://dx.doi.org/10.1118/1.4705346]

Key words: doxorubicin, focused ultrasound, HIFU, prostate cancer

I. INTRODUCTION

Pulsed high-intensity focused ultrasound (pFUS) is able to create acoustic cavitation (microbubbles) in the focused region of tissues. It has been suggested that these microbubbles can increase the permeability of the local vascular wall and cell membrane.[1–3] It is also suggested that radiation force may induce local tissue dilation and thus widen the interstitial space to enhance the interstitial transport.[3,4] Conventionally used for thermal ablation, high-intensity focused ultrasound was recently explored as a technique to enhance local drug delivery to tissues by using the pulse mode with low acoustic powers and duty cycles, which will maintain an insignificant local temperature elevation thus avoiding

thermal damage. For simplicity, the term "nonthermal" is used in this work to refer to this safe temperature working zone of pFUS in contrast to thermal ablation. With pFUS, energy is delivered and focused to the treatment target by ultrasound waves without invasion to normal tissues. With the guidance of magnetic resonance imaging or diagnostic ultrasound, accurate targeting can be achieved. Previous experiments on small animals have demonstrated that focused ultrasound exposure can enhance the delivery of different agents into tumors[4–8] or disrupt the local blood–brain barrier in a reversible way.[9,10] For example, Dromi *et al.*[6] used pFUS-induced mild temperature elevation (4–5 °C) to trigger Dox-loaded low-temperature-sensitive liposomes and thus enhance the delivery of doxorubicin (Dox) in a

11

mouse mammary tumor model. Hancock *et al.*[4] showed the enhanced delivery of a variety of fluorophores in the calf muscle of mice when combined with pFUS exposure, while Hynynen *et al.*[9] investigated the local and reversible blood–brain barrier disruption by noninvasive pFUS and looked at the suitable acoustic parameters for trans-skull sonications.

These preliminary studies used custom ultrasound devices that were tested in different animal tumor models. Although the results are promising, the translation of these techniques to clinical application requires extensive studies. Detailed studies are still necessary to examine the potential clinical applications of pFUS on other drugs and tumor types. Investigations of optimal pFUS parameters are also critical in order to maximize the enhancement of therapeutic agent uptake in treated tumor volumes. Developing quantitative methods to evaluate the pFUS enhancement would be necessary for such a systematic parametric study. Furthermore, MRI can be used for tumor delineation, treatment planning, and ultrasound beam placement with 1 mm accuracy. MRI is also used to monitor the therapeutic effects of pFUS in real time by monitoring the temperature changes using MR thermometry. The MR-guided pFUS technique is increasingly accepted and has been integrated in several clinical FUS systems such as ExAblate 2000 (InSightec Ltd., Tirat Carmel, Israel) and Sonalleve (Philips Healthcare, Andover, MA). Animal studies with these clinical devices would be useful to facilitate future preclinical evaluations.

In this study, Dox was delivered to prostate tumors with the aid of MR-guided pFUS. Dox has been chosen for this study as it inherits fluorescent substance that allows us to evaluate the effects of the pFUS treatment by measuring the drug concentration in the treated tumor volume quantitatively using a fluorometer,[11] and the spatial drug distribution can be viewed by fluorescent imaging. In addition, it is an anthracycline antibiotic used for treatment of a wide spectrum of malignancies including prostate cancers. Clinical trails of Dox are being conducted for prostate cancers, especially for hormone refractory diseases.[12–14] However, the effectiveness of Dox is limited due to its high toxicity and side effects such as alopecia, acute nausea, vomiting, stomatitis, and suppression of bone marrow.[15–17] Accumulative uptake by the heart may cause cardiotoxicity and heart failure.[16] Repeated administration may also lead to strong multidrug resistance response in tumor cells.[18] To reduce its toxicity and side effects, new strategies were proposed to reduce the normal tissue uptake or offset the side effects of Dox. For example, Dox was encapsulated in the liposome to prolong the circulation time, reduce normal tissue uptake, and enhance accumulation in tumors.[14,19] Treatment regimens combining Dox with other drugs such as sildenafil was also investigated to offset the side effects of Dox.[15] From a drug delivery viewpoint, enhancing the local uptake of Dox in prostate tumors would reduce the total dose needed for the same therapeutic efficacy and, therefore, reduce the toxicity and side effects.

The purpose of this study was to quantitatively investigate the effect of MR-guided pFUS on the uptake of Dox in prostate tumors *in vivo*. An orthotopic animal prostate tumor model was developed using a human LNCaP tumor cell line to best mimic a clinical scenario. A clinical FUS system, Insightec ExAblate 2000, which received FDA clearance for the treatment of uterine fibroids, was used with a 1.5T GE MR scanner for MR-guided pFUS treatment. We hypothesized that the enhancement of intratumoral uptake of Dox may improve tumor growth inhibition without increasing systemic toxicity or using lower doses to achieve the same treatment efficacy with reduced systemic side effects. This quantitative study will test the method for a future systemic parametric study to maximally enhance the tumor uptake. The results may also provide important preclinical data for the use of pFUS as a modality to enhance drug delivery for the treatment of prostate cancers.

II. MATERIALS AND METHODS

II.A. Study of the pFUS treatment parameters

In order to avoid potential thermal damage, a tissue phantom study was conducted to evaluate the pFUS-induced temperature elevation with various acoustic power and sonication duration. An approximately cylindrical tissue phantom (diameter = ~10 cm, length = ~13 cm) provided by the vendor (InSightec Ltd., Tirat Carmel, Israel) was used. The experiment setup was similar to the animal experiment described below (Fig. 1) except that a larger surface coil
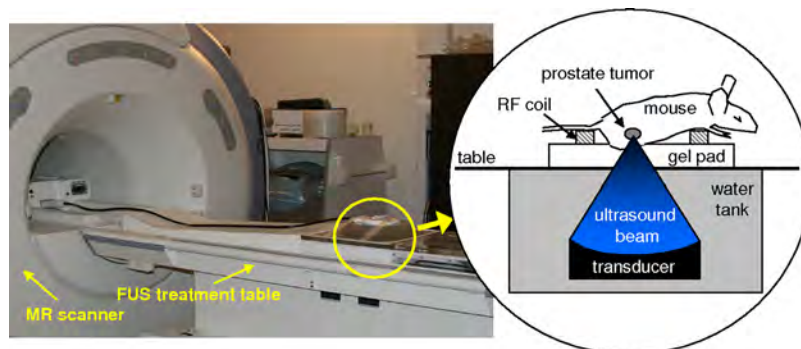

FIG. 1. Experimental setup for MR-guided pFUS exposure of prostate tumors in mice. The setup includes an MR scanner, pFUS treatment table, an acoustic gel pad, and a small RF surface coil. The mouse was in a prone position and the ultrasound beam was delivered from below. A small tissue phantom was also placed next to the mouse to verify the accuracy of the focal ultrasound delivery before treatment.

(diameter $= \sim 15$ cm) and a tissue phantom were used. The tissue phantom was manufactured by ATS Labs, Inc. (Bridgeport, CT) with acoustic properties similar to those of human soft tissue (the attenuation coefficient $= 0.503$ dB cm^{-1} MHz^{-1}; speed of sound $= 1538$ MPS; estimated specific heat $= 2.684$ cal/g). With the given duty cycle of 10%, pulse rate 1 Hz, and acoustic frequency 1 MHz, the phantom was sonicated with various acoustic powers ranging from 10 to 50 W and sonication durations ranging from 10 to 60 s in 10 W and 10 s increments, respectively. The temperature elevations in the focal zone were measured for each pair of parameters (i.e., acoustic power and sonication duration) using MR thermometry, which is a machine built-in software function. The relation of the temperature elevation to acoustic power and exposure duration was plotted by bilinearly interpolating the measured data.

II.B. Orthotopic prostate tumor model

An animal prostate tumor model was developed by implanting human prostate cancer LNCaP cells in the prostates of nude mice. The cells were obtained from the American Type Culture Collection (ATCC) and cultured in Dulbecco's modified Eagle's medium (DMEM)-F12 medium, containing 10% fetal bovine serum (FBS), 1% L-glutamine, and 1% penicillin–streptomycin as described previously.[8,20] Male athymic Balb/c nude mice (6 weeks old) were purchased from Harlan (Indianapolis, IN). Animal studies were carried out in compliance with a protocol approved by the Institutional Animal Care and Use Committee (IACUC) of Fox Chase Cancer Center (FCCC). Aseptic techniques were used for injection of LNCaP cells in the prostates of nude mice as described previously.[8] Nude mice were anesthetized using methoxyflurane. A lower midline incision was made above the presumed location of the bladder. The dorsal prostate lobes were exposed and 1×10^6 LNCaP cells in 25 μl volume were injected with a 30-gauge needle. The incision was sealed by suturing the muscle layer and using two–three wound clips for the skin layer. Buprenorphine was given immediately after the tumor implantation for pain relief.

II.C. MR-guided pFUS exposure

The prostate tumor volume was monitored weekly after tumor implantation using a 1.5T GE MR scanner (GE Healthcare, Waukesha, WI). Animals were anesthetized for MR scanning with an intramuscular (i.m.) injection of a mixed solution of ketamine (60 mg/kg) and acepromazine (2.5 mg/kg) in 15 μl volume. A 15-min anesthesia was required to immobilize the animal during MR scanning. When the prostate tumor volume reached approximately 100 mm^3, treatment was initiated. Tumor-bearing mice were randomly assigned to one of the three experimental groups ($n = 8$/group): (1) Dox following pFUS exposure (pFUS + DOX group), (2) Dox only (DOX group), and (3) a control group. MR-guided pFUS treatment was performed using the ExAblate 2000 (InSightec Ltd., Tirat Carmel, Israel) with a 1.5T GE MR scanner. Figure 1 shows the experimental setup. Animals were anesthetized for the pFUS treatment with ketamine and acepromazine in 30 μl

volume i.m. and placed on an acoustic gel pad, which was laid on the FUS treatment table. Caution was taken to ensure that the mouse, the acoustic gel, and the treatment table were well coupled acoustically to avoid the formation of air bubbles. A ring-shaped surface coil (diameter $= \sim 8$ cm) was used for the MR signal detection. T2-weighted MR images were acquired using a fast-recovery fast spin-echo (FRFSE) sequence with parameters: TR/TE $= 2200/85$ ms, NEX $= 3$, matrix $= 288 \times 288$, FOV $= 7 \times 7$ cm^2 (resolution $= 0.243 \times 0.243$ mm^2), and slice thickness $= 2$ mm. Both coronal and axial scans were performed and the acquired MR images were loaded immediately into the FUS treatment planning system for treatment planning (Fig. 2).

Nonthermal sonications were delivered by keeping the body temperature below 42 °C. The body temperature during sonication was monitored in real time (~ 3 s delay) by MR thermometry using a temperature-induced proton resonance frequency shift method. MR thermometry scans were acquired using a fast spoiled gradient echo (FSGR) sequence with parameters: TR/TE $= 25.9/12.8$ ms, flip angle $= 30°$, NEX $= 1$, number of echo $= 1$, FOV $= 22 \times 22$ cm^2, matrix $= 256 \times 128$, and slice thickness $= 3$ mm. Tumor-bearing mice from group 1 were exposed to pFUS using the following parameters: 1 MHz ultrasound, 25 W acoustic power, and 1 Hz pulse rate with a 10% duty cycle for 60 s for each sonication spot. During the pFUS treatment, temperature elevations between 4 and 5 °C were observed under these pFUS parameters. The focal length was 98–102 mm and the aperture of pFUS transducer was 12 cm. The ultrasound focal zone is an elongated ellipsoid with a longitudinal length of 6.8 mm (-3 dB) and a radial diameter of 1.25 mm (-3 dB). The estimated peak-negative pressure in the focal zone was 7.8 MPa and the average acoustic intensity was 20.4 W/mm^2. A total of four–eight sonication spots were used to cover the entire tumor volume depending on the tumor size. The pFUS parameters were selected based on our tissue phantom study. Tail vein injections (volume of 100 μl) of Dox (10 mg/kg) were given to mice in group 1 immediately after pFUS exposure (within 10 min). Group 2 received the same Dox injection, but without pFUS exposure. No Dox injection was given to the control animals.

II.D. Assay for intratumoral doxorubicin content

Mice were euthanized 2 h after the Dox injection assuming the drug had circulated into the prostate tumor. Prostate tumors were excised, weighed, and homogenized in Eppendorf 1.5 ml tubes. A lysis buffer (800 μl) containing 3% hydrochloride, 48.5% ethanol, and 48.5% double-distilled water was added to tissue homogenates, vortexed, and stored in the dark at 4 °C overnight. The next day the lysates were centrifuged at 5000 rpm for 10 min at 4 °C and supernatants were collected. Three 100 μl supernatant aliquots from each sample were placed in 96-well plates and read with a Fluoroskan Ascent microplate fluorometer and luminometer (excitation at 485 nm; emission at 538 nm; Thermo Fisher Scientific, Waltham, MA). Fluorescence readings were compared with values from a standard calibration curve. The
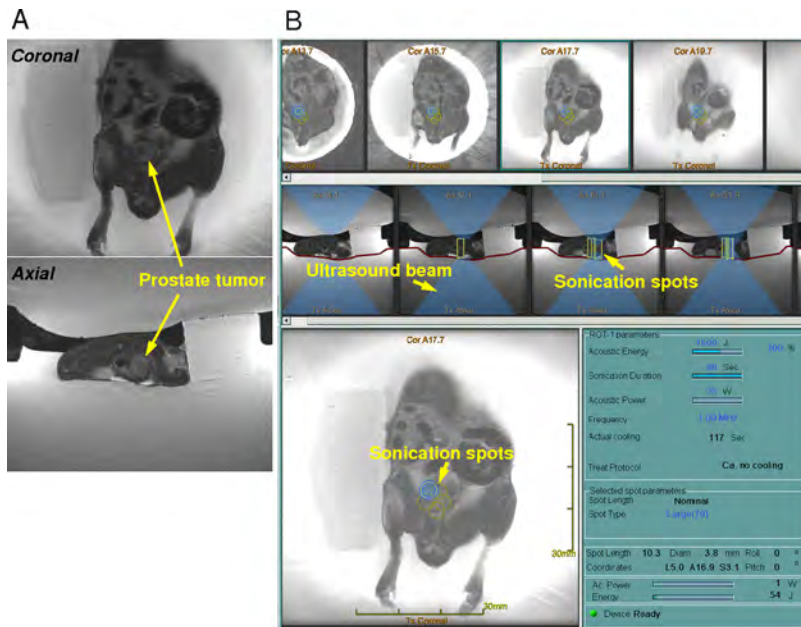
Ma, Chang Ming (Charlie)   2783

FIG. 2. (a) MR coronal and axial views of a typical mouse prostate tumor for pFUS treatment. (b) Real-time treatment planning based on acquired MR images (top: coronal view of sonication spot distribution; middle: axial view of ultrasound beam passing through the tumor and the surrounding materials; bottom: a zoomed coronal view of sonication spots covering the mouse prostate tumor). Planned sonication spots had a cylindrical shape with a diameter of 3.8 mm and a length of 10.3 mm.

calibration curve comprised serial dilutions of Dox and related the fluorescence readings to the Dox mass [Fig. 4(a)]. The total amount of Dox in each tumor sample was normalized to its weight and expressed as microgram of Dox per gram of tumor weight. Fluorescence values of the control samples were subtracted as background.

II.E. Light and fluorescence microscopy analysis

A separate experiment was conducted to compare the Dox distribution in the tumor tissue with and without pFUS treatment using fluorescence microscopy. Five tumor-bearing mice were used for this experiment; two received pFUS and Dox as described above, and two received Dox only. One animal received no treatment and was used for determination of the background levels of fluorescence in the tissue. Two hours following the treatment, animals were euthanized, tumors were harvested, snap frozen in liquid nitrogen, and cut into frozen sections using Leica CM1850 cryostat (Leica Microsystems GmbH, Wetzlar, Germany). Tumor sections were examined using the Eclipse600 microscope (Nikon Instruments, Inc., Melville, NY) to determine the difference of the spatial Dox distribution among various groups.

An additional experiment was conducted to compare histological changes between pFUS-treated prostate tumors ($n = 3$) and control, untreated tumors ($n = 3$) using light microscopy. Tumor-bearing mice were given the same pFUS exposures as described above and euthanized within 30 min of treatment. Prostate tumors were removed, fixed in 10% neutral buffered formalin, and embedded in paraffin. Paraffin blocks were used to generate the hematoxylin and eosin (H&E)-stained sections. Slides were examined using a light microscope (Nikon) to observe histological changes after pFUS treatment.

II.F. Statistical analysis

Measured tumor Dox concentrations were analyzed statistically. The mean and standard deviation of the mean (SEM) were calculated and the results were expressed as *mean ± SEM*. To determine if there was a significant difference between treated and control groups, Student's *t*-test was used and a *p*-value ≤ 0.05 was considered to be significant.

III. RESULTS

III.A. pFUS-induced temperature elevation

Figure 3 shows the pFUS-induced temperature elevation based on the tissue phantom study using our experimental pFUS system (at acoustic frequency 1 MHz, duty cycle 10%, and pulse rate 1 Hz). Assuming that biological tissues are not damaged below $42\,°C$, Fig. 3 suggested that at 25 W acoustic power the exposure duration of 60 s would be safe to avoid tissue damage (assuming a normal body temperature of $37\,°C$ and a $<5\,°C$ temperature elevation). It can be seen that the temperature increases exponentially with the acoustic power and the acoustic power and sonication duration follow an inverse relationship. When delivering the same acoustic energy at a lower acoustic power, a lower temperature increase was observed due to heat loss.

III.B. Quantitative measurement of Dox uptake in prostate tumor

Comparison of the Dox concentration in prostate tumors between mice treated with pFUS (pFUS + DOX) and without (DOX alone) showed a significant increase in Dox uptake in treated tumors (Fig. 4). Dox concentration in the pFUS-treated group was 14.9 ± 2.5 μg/g, while in the Dox only group it was 9.5 ± 1.6 μg/g. The difference between these two groups was statistically significant ($p = 0.05$). There was an approximately 60% increase of Dox uptake in the prostate tumors exposed to pFUS with the parameters used in this study. These results were consistent with our previous studies on Docetaxel.[8]
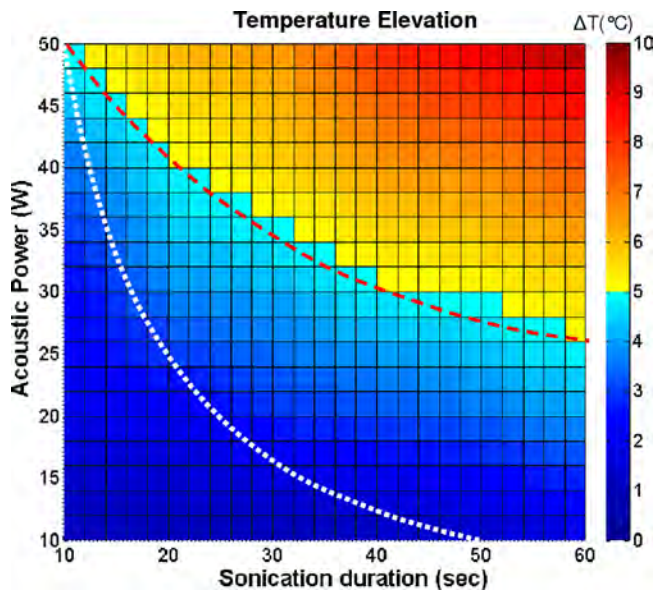
14

FIG. 3. pFUS-induced temperature elevation using different acoustic powers and sonication durations based on the tissue phantom measurement (acoustic frequency: 1 MHz; duty cycle: 10%; pulse rate: 1 Hz). The red dashed line indicates a 5 °C temperature elevation, which will increase the body temperature to 42 °C, assuming a normal body temperature of 37 °C. The white dotted line indicates the same acoustic energy delivered using different acoustic power and the temperature elevation changes.

III.C. Spatial Dox distribution in prostate tumor

The enhancement of Dox uptake in pFUS-treated tumors was confirmed by fluorescence microscopy. Figure 5 shows typical fluorescence micrographs of prostate tumor tissues from the three different groups, i.e., control, Dox injection only, and Dox injection after pFUS treatment. More Dox signals (emission from Dox) were observed in pFUS-treated tumor tissues compared to those without pFUS treatment. Images also show the inhomogeneous distribution of Dox in prostate tumor tissues. The observed distribution was consistent with findings of enhanced Dox uptake quantitatively measured using the fluorescence technique (Fig. 4).

III.D. Histology analysis

Figure 6 shows histological changes in prostate tumors with and without pFUS treatment. A significant increase in the blood cell extravasation was observed in the pFUS-treated tumors compared with those without the pFUS treatment. There were no implosion cysts[21] observed in the tumor tissues, indicating that no thermal damage occurred as was observed in thermal ablation. The increase in the blood extravasations demonstrated the increased permeability of blood vessels in the tumor tissues. Other histological changes such as extracellular matrix disintegration or increased intracellular spacing were not clearly evident.

IV. DISCUSSION

Previous studies by other groups have demonstrated that pulsed focused ultrasound can enhance local drug uptake in tumors. These preliminary studies used either a custom-
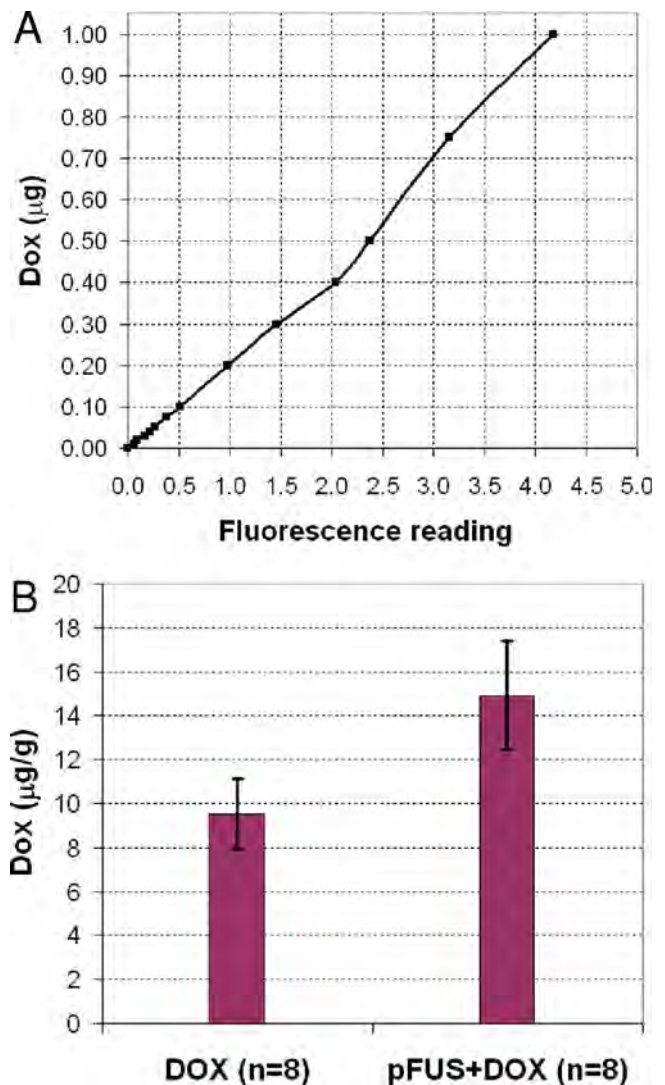

FIG. 4. (a) The doxorubicin fluorescence calibration curve showing the fluorescence readings for different mass of Dox. (b) Comparison of tumor Dox concentration between untreated (DOX) and pFUS-treated groups (pFUS + DOX). Tumor Dox concentration is defined as microgram of Dox per gram of tumor weight. In the pFUS + DOX group, it was 14.9 ± 2.5 μg/g, while in the DOX-only group it was 9.5 ± 1.6 μg/g ($p = 0.05$).

made ultrasound device or different animal models.[4–7,22] Detailed studies are necessary to investigate the potential clinical applications of pFUS for individual drugs and tumor types. For example, drug transport into tumor tissues is affected by several factors, including agent permeability across the blood vasculature and microenvironment difference between various types of tumors, such as interstitial fluid pressure and tumor cell density.[23] On the other hand, tumor microenvironment changes induced by pFUS are most likely related to the treatment parameters used and also related to physical properties of the tumor itself. In this study, we quantitatively investigated the doxorubicin uptake in the prostate tumor with the aid of MR-guided pFUS. The orthotopically implanted mouse prostate tumor model was used to best mimic a clinical scenario. A commercially available clinical MR-guided pFUS system was used, which is currently under investigation for its clinical use for pFUS-
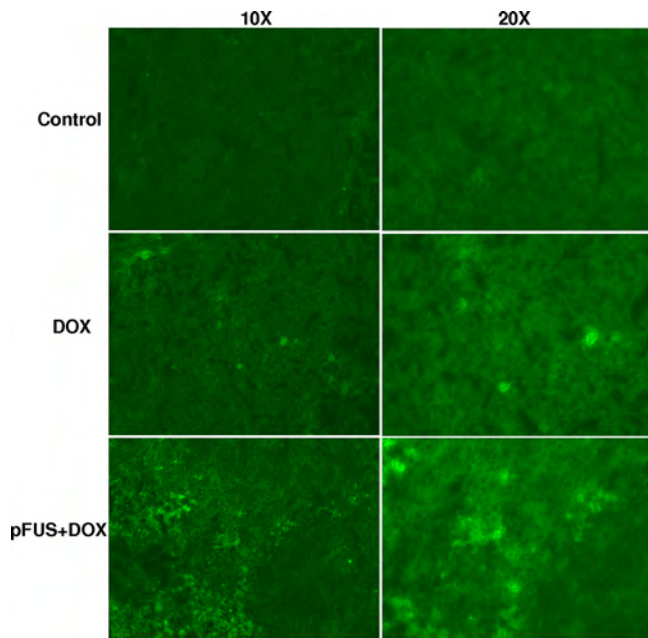
FIG. 5. Fluorescence photomicrographs of the Dox distribution in prostate tumors for different groups (control, DOX: Dox injection only; pFUS + DOX: Dox injection after pFUS treatment). Images were acquired with a magnification of $10\times$ (left column) and $20\times$ (right column).

enhanced drug delivery. Our study showed that pFUS exposures significantly enhanced the uptake of Dox in prostate tumors with increased blood extravasation.

The interactions between pFUS and tissues lead to several effects including mild temperature elevation due to local energy absorption, cavitation due to sufficiently low fluid pressure, and tissue strain due to radiation force. Previous mechanistic studies of pFUS enhancing effects suggested that the temperature elevation has no significant contribution to the delivery enhancement.[24] Instead, it is more likely due to the cavitation and radiation force that induce changes of local tissue properties such as increased vascular permeability and interstitial transport. In murine calf muscle exposed to pFUS, cavitation was detected using an *in vivo* monitoring technique.[24] Enlarged gaps between mice muscle fibers exposed to pFUS were clearly observed immediately or even 24 or 48 h after the pFUS treatment.[4] Extravasation was evident in several previous pFUS enhancement studies[4,7,24] as well as in this study. From a biomechanics viewpoint, the acoustic intensity or pressure applied on the tissue plays a major role in cavitation and radiation force and may directly determine the types of bioeffects. Previous pFUS studies

have used various acoustic intensities ranging from ~2.2,[8] ~11.1,[7] ~13.7,[6,7,25] to ~26.6 W/mm^2 (Refs. 4, 24, and 26) for different tissues such as tumors and muscle. While different levels of pFUS enhancing effects were observed, it is not clear which acoustic intensity will give the maximal enhancement. A systematic parametric study using different acoustic intensities would be necessary in future studies.

Practically, several issues must be investigated for the use of pFUS as a modality to mediate the drug delivery to tumors, such as the acoustic power, focal spot temperature, and time point of drug injection. The temperature elevation at the focal spot is affected by several factors including the energy input rate, temperature gradient to surrounding region, and thermal transfer coefficient of the material. Increasing the energy input rate will increase temperature of the focal zone while a large temperature gradient and thermal transfer coefficient will increase the thermal flux out of the focal zone and decrease the temperature. The balance between the acoustic power and the heat loss in the focal zone determines the temperature elevation. As a result, higher temperature elevation was observed when using higher acoustic power, even though the total energy delivered did not change as seen in Fig. 3. In addition, a higher acoustic power of 25 W was used to enhance the Dox uptake in tumor which has an estimated peak-negative pressure of 7.8 MPa in the focal zone. Increasing the acoustic power will increase the pressure at the focal zone, which may finally lead to increased interstitial space and vessel wall opening and enhance drug uptake in tumors. However, in order to keep the final body temperature at a safe level, the option to increase power is limited due to the increased temperature as shown in Fig. 3. Higher pressure also has a tendency to induce other effects such as eruption of microbubbles.[1] The time point of drug injection may also play an important role in optimal drug delivery enhancement. In this study, drug was injected i.v. immediately after the pFUS exposure. For clinical applications, this could be done simultaneously with the pFUS exposure or at different time points to achieve a better uptake.

The results from this study are consistent with our previous study of enhanced [^{3}H]-docetaxel uptake in prostate tumors, where a lower acoustic power (4 W), higher duty cycle (50%), and pulse rate (5 Hz) were used for pFUS treatment with the same clinical MR-guided FUS system.[8] While the drug transport properties might differ between Dox and Docetaxel, enhanced uptake was observed in both studies with different data analysis tools. In this study, Dox was used for quantitative study by taking advantage of its fluorescence properties. Dox
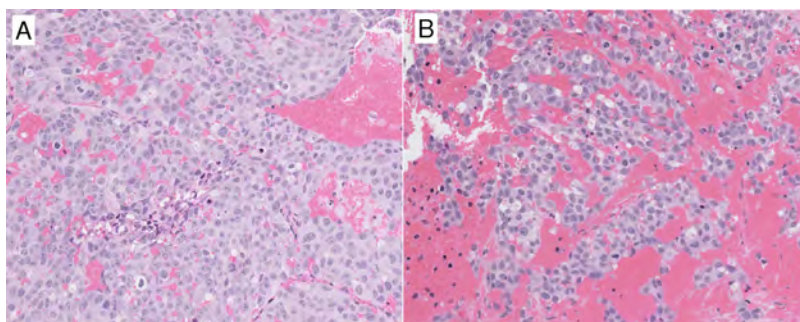

FIG. 6. H&E staining of mouse prostate tumor without pFUS treatment (a) and with pFUS treatment (b) ($\times 20$). Note the increased extravasation of blood cells in the pFUS-treated tumor.

also has a relatively long circulation time which allows sufficient plasma Dox concentration for the delivery enhancement study. According to the previous studies on humans and mice,[19,27,28] the terminal half-life of Dox was approximately 25–30 h. The level of pFUS enhancing effects may be determined by pFUS parameters. Specific pFUS parameters may exist to maximize the drug uptake enhancement, and further studies are needed to investigate such optimal pFUS parameters for maximal Dox uptake. This study provides a quantitative method for such systematic studies.

This study showed that Dox uptake in prostate tumors can be enhanced significantly by nonthermal pFUS. These results demonstrate the clinical potential of pFUS-mediated drug delivery for prostate tumor treatment. By enhancing the local Dox uptake in tumors, lower doses could be used to achieve the same treatment efficiency while significantly reducing its side effects, leading to improved quality of patient care. In addition, tumors exposed to pFUS with similar parameters also showed significant tumor growth delay.[29] As a result, pFUS may not only enhance the local drug uptake but also cause additional tumor cell killing. These combined effects may provide a promising modality for prostate cancer therapy. Future studies should be designed to investigate the optimal pFUS parameters and treatment regimens to achieve the maximal therapeutic effect.

ACKNOWLEDGMENTS

[a]Author to whom correspondence should be addressed. Electronic mail: lili.chen@fccc.edu; Telephone: 215-728-3003; Fax: 215-728-4789.

[1]C. C. Coussios and R. A. Roy, "Applications of acoustics and cavitation to noninvasive therapy and drug delivery," Annu. Rev. Fluid Mech. **40**, 395–420 (2008).

[2]J. E. Kennedy, "High-intensity focused ultrasound in the treatment of solid tumours," Nat. Rev. Cancer **5**, 321–327 (2005).

[3]V. Frenkel, "Ultrasound mediated delivery of drugs and genes to solid tumors," Adv. Drug Delivery Rev. **60**, 1193–1208 (2008).

[4]H. A. Hancock, L. H. Smith, J. Cuesta, A. K. Durrani, M. Angstadt, M. L. Palmeri, E. Kimmel, and V. Frenkel, "Investigations into pulsed high-intensity focused ultrasound-enhanced delivery: Preliminary evidence for a novel mechanism," Ultrasound Med. Biol. **35**, 1722–1736 (2009).

[5]V. Frenkel, A. Etherington, M. Greene, J. Quijano, J. W. Xie, F. Hunter, S. Dromi, and K. C. P. Li, "Delivery of liposomal doxorubicin (Doxil) in a breast cancer tumor model: Investigation of potential enhancement by pulsed-high intensity focused ultrasound exposure," Acad. Radiol. **13**, 469–479 (2006).

[6]S. Dromi, V. Frenkel, A. Luk, B. Traughber, M. Angstadt, M. Bur, J. Poff, J. W. Xie, S. K. Libutti, K. C. P. Li, and B. J. Wood, "Pulsed-high intensity focused ultrasound and low temperature sensitive liposomes for enhanced targeted drug delivery and antitumor effect," Clin. Cancer Res. **13**, 2722–2727 (2007).

[7]E. L. Yuh, S. G. Shulman, S. A. Mehta, J. W. Xie, L. L. Chen, V. Frenkel, M. D. Bednarski, and K. C. P. Li, "Delivery of systemic chemotherapeutic agent to tumors by using focused ultrasound: Study in a murine model," Radiology **234**, 431–437 (2005).

[8]L. L. Chen, Z. M. Mu, P. Hachem, C. M. Ma, A. Wallentine, and A. Pollack, "MR-guided focused ultrasound: Enhancement of intratumoral uptake of H-3-docetaxel *in vivo*," Phys. Med. Biol. **55**, 7399–7410 (2010).

[9]K. Hynynen, N. McDannold, N. A. Sheikov, F. A. Jolesz, and N. Vykhodtseva, "Local and reversible blood-brain barrier disruption by noninvasive focused ultrasound at frequencies suitable for trans-skull sonications," Neuroimage **24**, 12–20 (2005).

[10]L. H. Treat, N. McDannold, N. Vykhodtseva, Y. Z. Zhang, K. Tam, and K. Hynynen, "Targeted delivery of doxorubicin to the rat brain at therapeutic levels using MRI-guided focused ultrasound," Int. J. Cancer **121**, 901–907 (2007).

[11]M. Gigli, S. M. Doglia, J. M. Millot, L. Valentini, and M. Manfait, "Quantitative study of doxorubicin in living cell-nuclei by microspectrofluorometry," Biochim. Biophys. Acta **950**, 13–20 (1988).

[12]R. Petrioli, A. I. Fiaschi, E. Francini, A. Pascucci, and G. Francini, "The role of doxorubicin and epirubicin in the treatment of patients with metastatic hormone-refractory prostate cancer," Cancer Treat Rev. **34**, 710–718 (2008).

[13]A. Heidenreich, F. Sommer, C. H. Ohimann, A. J. Schrader, P. Olbert, J. Goecke, and U. H. Engelmann, "Prospective randomized phase II trial of pegylated doxorubicin in the management of symptomatic hormone-refractory prostate carcinoma," Cancer **101**, 948–956 (2004).

[14]K. A. Harris, E. Harney, and E. J. Small, "Liposomal doxorubicin for the treatment of hormone-refractory prostate cancer," Clin. Prostate Cancer **1**, 37–41 (2002).

[15]A. Das, D. Durrant, C. Mitchell, E. Mayton, N. N. Hoke, F. N. Salloum, M. A. Park, I. Qureshi, R. Lee, P. Dent, and R. C. Kukreja, "Sildenafil increases chemotherapeutic efficacy of doxorubicin in prostate cancer and ameliorates cardiac dysfunction," Proc. Natl. Acad. Sci. U.S.A. **107**, 18202–18207 (2010).

[16]P. Singal, T. M. Li, D. Kumar, I. Danelisen, and N. Iliskovic, "Adriamycin-induced heart failure: Mechanisms and modulation," Mol. Cell. Biochem. **207**, 77–86 (2000).

[17]E. Rivera, "Liposomal anthracyclines in metastatic breast cancer: Clinical update," Oncologist **8**, 3–9 (2003).

[18]F. Shen, S. Chu, A. K. Bence, B. Bailey, X. Xue, P. A. Erickson, M. H. Montrose, W. T. Beck, and L. C. Erickson, "Quantitation of doxorubicin uptake, efflux, and modulation of multidrug resistance (MDR) in MDR human cancer cells," J. Pharmacol. Exp. Ther. **324**, 95–102 (2008).

[19]A. Gabizon, R. Catane, B. Uziely, B. Kaufman, T. Safra, R. Cohen, F. Martin, A. Huang, and Y. Barenholz, "Prolonged circulation time and enhanced accumulation in malignant exudates of doxorubicin encapsulated in polyethylene-glycol coated liposomes," Cancer Res. **54**, 987–992 (1994).

[20]Z. Mu, P. Hachem, H. Hensley, R. Stoyanova, H. W. Kwon, A. L. Hanlon, S. Agrawal, and A. Pollack, "Antisense MDM2 enhances the response of androgen insensitive human prostate cancer cells to androgen deprivation *in vitro* and *in vivo*," Prostate **68**, 599–609 (2008).

[21]L. L. Chen, I. Rivens, G. Terhaar, S. Riddler, C. R. Hill, and J. P. M. Bensted, "Histological-changes in rat-liver tumors treated with high-intensity focused ultrasound," Ultrasound Med. Biol. **19**, 67–74 (1993).

[22]K. Hynynen, "Focused ultrasound for blood-brain disruption and delivery of therapeutic molecules into the brain," Expert Opin. Drug Deliv. **4**, 27–35 (2007).

[23]R. K. Jain, "Delivery of molecular and cellular medicine to solid tumors," J. Controlled Release **53**, 49–67 (1998).

[24]B. E. O'Neill, H. Vo, M. Angstadt, K. P. C. Li, T. Quinn, and V. Frenkel, "Pulsed high intensity focused ultrasound mediated nanoparticle delivery: Mechanisms and efficacy in murine muscle," Ultrasound Med. Biol. **35**, 416–424 (2009).

[25]K. M. Dittmar, J. W. Xie, F. Hunter, C. Trimble, M. Bur, V. Frenkel, and K. C. P. Li, "Pulsed high-intensity focused ultrasound enhances systemic administration of naked DNA in squamous cell carcinoma model: Initial experience," Radiology **235**, 541–546 (2005).

[26]A. Khaibullina, B. S. Jang, H. Sun, N. Lee, S. Yu, V. Frenkel, J. A. Carrasquillo, I. Pastan, K. C. P. Li, and C. H. Paik, "Pulsed high-intensity focused ultrasound enhances uptake of radiolabeled monoclonal antibody to human epidermoid tumor in nude mice," J. Nucl. Med. **49**, 295–302 (2008).

[27]R. F. Greene, J. M. Collins, J. F. Jenkins, J. L. Speyer, and C. E. Myers, "Plasma pharmacokinetics of adriamycin and adriamycinol—Implications for the design of invitro experiments and treatment protocols," Cancer Res. **43**, 3417–3421 (1983).

[28]K. M. Laginha, S. Verwoert, G. J. R. Charrois, and T. M. Allen, "Determination of doxorubicin levels in whole tumor and tumor nuclei in murine breast cancer tumors," Clin. Cancer Res. **11**, 6944–6949 (2005).

[29]C. M. Ma, D. Cvetkovic, X. Chen, and L. Chen, "Non-thermal pulsed focused ultrasound for cancer therapy," Med. Phys. **38**, 3824–3824 (2011).